Received: 9 July 2019 | Revised: 16 September 2019 | Accepted: 22 September 2019

DOI: 10.1002/mds3.10047

RESEARCH ARTICLE

MEDICAL DEVICES & SENSORS WILEY

Biosensor based on the directly enzyme immobilization into a gold nanotriangles/conductive polymer biocompatible coat for electrochemical detection of Chlorpyrifos in water

Karla Ramírez-Sánchez[1] | Fernando Alvarado-Hidalgo[2] | Roy Zamora-Sequeira[1] | Giovanni Sáenz-Arce[3] | Oscar Rojas-Carrillo[4] | Esteban Avedaño-Soto[5] | Clemens Ruepert[6] | Freylan Mena-Torres[6] | Ricardo Starbird-Pérez[1]

[1]Centro de Investigación y de Servicios Químicos y Microbiológicos CEQIATEC, Escuela de Química, Instituto Tecnológico de Costa Rica, Cartago, Costa Rica

[2]Master Program in Medical Devices Engineering, Instituto Tecnológico de Costa Rica, Cartago, Costa Rica

[3]Departamento de Física, Universidad Nacional, Heredia, Costa Rica

[4]Escuela de Química, Universidad Nacional, Heredia, Costa Rica

[5]Departamento de Física, Centro de Investigación en Ciencia e Ingeniería de Materiales (CICIMA), Universidad de Costa Rica, San Pedro, Costa Rica

[6]Central American Institute for Studies on Toxic Substances (IRET), Universidad Nacional, Heredia, Costa Rica

Correspondence
Roy Zamora-Sequeira and Ricardo Starbird-Pérez Centro de Investigación y de Servicios Químicos y Microbiológicos CEQIATEC, School of Chemistry, Instituto Tecnológico de Costa Rica, 159-7050, Costa Rica
Emails: rzamorasequeira@ina.ac.cr; rstarbird@itcr.ac.cr

Funding information
CONARE FEES, Grant/Award Number: 08-2018; Instituto Tecnológico de Costa Rica (ITCR)

Abstract

Organic conductive polymers have been widely used as active layers in bioelectronic devices. In this work, a novel approach to entrap enzymes directly into the conductive active layer is described, using a polysaccharide as a surfactant. The surfactant allowed the electropolymerization from a micellar media and it acted as a doping agent in the conductive polymer. Gold nanotriangles were added to the matrix in order to enhance the enzymatic product quantification. The composition and oxidation state of the biocompatible conductive layer were confirmed by infrared spectrophotometric and Raman studies. Meanwhile, the gold nanotriangles presence, distribution and electrochemical activity were studied by transmission electron microscopy, atomic force microscopy, dynamic light scattering and cyclic voltammetry techniques. The inhibition of the enzyme, due to the presence of pesticides, was used to electrochemically quantify their concentration in real water samples. The concentration was confirmed by gas and liquid chromatography. Therefore, this novel composite active layer allows building a biosensor with suitable performance for an early warning in environmental control, especially in countries highly impacted by agricultural activities.

KEYWORDS

acetylcholinesterase, biosensors, Chlorpyrifos, gold nanotriangles, κ-carrageenan

1 | INTRODUCTION

The worldwide use of pesticides has rapidly increased over the last decades, mainly in agriculturally based countries, and Costa Rica is among them (Food and Agriculture Organization, 2017). The presence of organophosphorus pesticides (e.g. Chlorpyrifos) is considered harmful due to activity inhibition of acetylcholinesterase enzyme (AChE) preventing the hydrolysis of the neurotransmitter acetylcholine (Dorraki, Safa, Jahanfar, Ghomi, & Ranaei-Siadat, 2015; Stoilova et al., 2010). AChE-based biosensors have been widely applied for the electrochemical detection of environmental pollutants (Du, Chen, Cai, & Zhang, 2007; Kok & Hasirci, 2004; Schulze, Schmid, & Bachmann, 2004; Sun & Wang, 2010), among several reasons this is due to their simplicity, high sensitivity, selectivity, rapid response and low cost (Du et al., 2007; Liu, Su, et al., 2011).

Conductive polymers are a new generation of smart materials in bioelectronics with a wide spectrum of applications (Goding, Gilmour, Martens, Poole-Warren, & Green, 2015; Kim et al., 2007; Mandal, Bhattacharjee, Chattopadhyay, & Bandyopadhyay, 2019; Mantione, Agua, Sanchez-Sanchez, & Mecerreyes, 2017; Starbird, Bauhofer, Meza-Cuevas, & Krautschneider, 2012). Poly (3,4-ethylenedioxythiophene) (PEDOT) is a conductive polymer used as a coat in sensors due to its biocompatibility, electrical conductivity, processing versatility, and its stability has been confirmed in previous investigations through induced electrochemical stress (Hernandez-Suarez, Ramirez, Alvarado, Avendano, & Starbird, 2019; Kaur, Adhikari, Cass, Bown, & Gunatillake, 2015). The conductive polymer allows the immobilization of biologically active structures in order to target molecules to the specific binding or interactions between biomaterials (Wang, Akiba, & Anzai, 2017). κ-carrageenan (κC) is a sulphonated polysaccharide that has been used for the electrochemical polymerization of PEDOT through a micellar system since the biopolymer provides an appropriate environment for the monomer dispersion, while acting as a doping agent in the conductive coating during the application (Hernandez-Suarez et al., 2019; Ren, Gong, Zeng, Guo, & Shen, 2016; Zamora-Sequeira, Ardao, Starbird, & García-González, 2018).

Gold nanoparticles (AuNPs) have emerged as promising materials for electrode modification, based on their high electrical conductivity, biocompatibility and affinity to different biomolecules (Pumera, 2014; Wang et al., 2017). In our system, gold nanotriangles (AuNTs) have been added as an electrochemical mediator for the electrochemical oxidation of acetylcholine, a substance produced during the AChE enzymatic activity, because of its well-reported affinity (Koryta & Pradáč, 1968).

In this work, the acetylcholinesterase enzyme was entrapped directly into a conductive PEDOT/κC/AuNTs coat for application as a biosensor. As far as known, the entrapment of AChE directly in the conductive polymer along with AuNTs and using κC as biocompatible doping agent has not been previously reported. The characterization of the coat confirmed the composition, distribution and electrochemical activity of the biosensor. The immobilized enzyme enables the construction of biosensors suitable for the selective detection of organophosphorus pesticides, including Chlorpyrifos, in real samples. Finally, the quantification of the acetylcholinesterase inhibition is an indicator of exposure to organophosphorus pesticides, particularly important for medical and environmental applications.

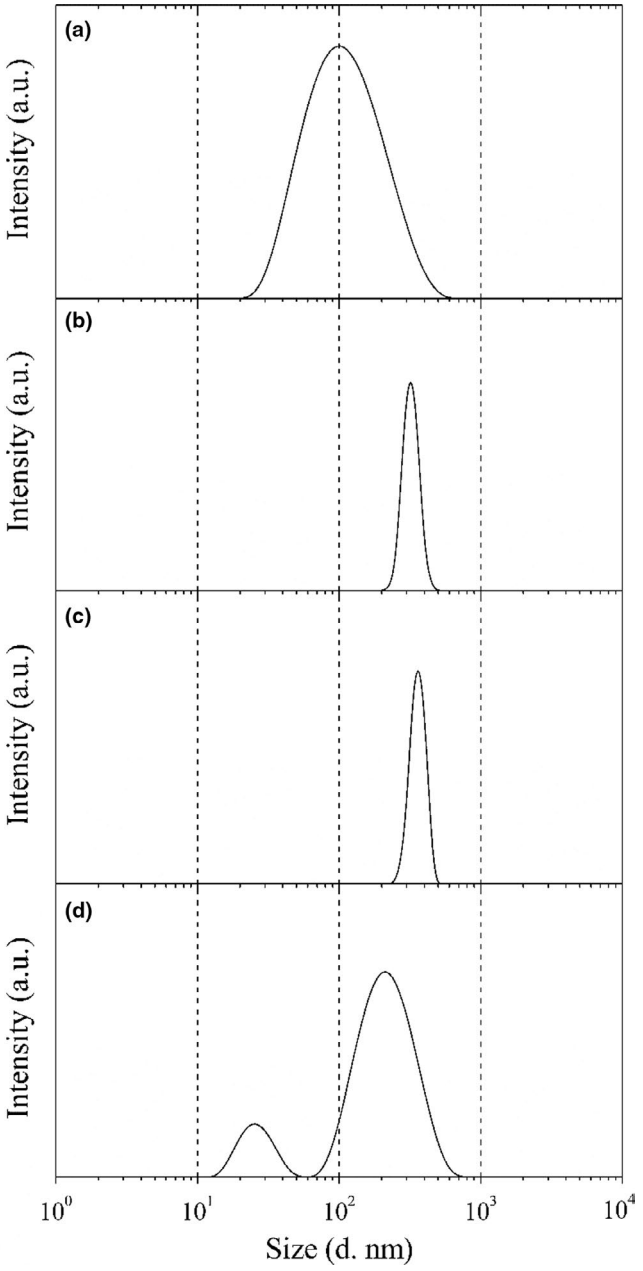

FIGURE 1 Size distribution (d.nm) of (a) Gold nanotriangles, (b) κ-carrageenan, (c) κ-carrageenan/EDOT and (d) κ-carrageenan/EDOT/AuNTs dispersion measured by DLS technique

2 | RESULTS AND DISCUSSION

2.1 | Characterization

2.1.1 | Synthesis and characterization of gold nanotriangles

The AuNTs were prepared using a green-chemistry vesicle phase, formed by phospholipids mixture in water in the absence of an external reducing agent. The mechanism of formation of the resulting nanoparticle was explained in terms of the Oswald ripening growth (Liebig, Thünemann, & Koetz, 2016). Triangular shape and size of the nanoparticles were previously described using transmission electron microscopy (TEM) and UV-visible spectroscopy (Bollella et al., 2019). In this work, the average hydrodynamic diameter of the purified AuNTs, evaluated by dynamic light scattering (DLS), was around 100 nm (see Figure 1a) and they showed a negative zeta potential of −60 mV. The size and shape of the AuNTs, incorporated into the conductive polymer coating, were confirmed by TEM and atomic force microscopy (AFM).

2.1.2 | Synthesis and characterization of conductive coat

The electrodes were modified by electrodeposition from a biocompatible dispersion (e.g., EDOT/κC/AuNTs). The κC system provides a homogenous environment to disperse the monomer, nanoparticles and the enzyme. The dispersion was evaluated in order to determine its stability, the size of particles and their aggregates.

The ζ-potential analysis confirmed the stability of the κ-carrageenan dispersion (−42 mV). The negative potential is a result of the anionic nature of the κC, and it is similar to the result previously reported (Hernandez-Suarez et al., 2019). The value shows no significant change when the monomer (EDOT) was added to the dispersion (−41 mV). Furthermore, the system κC/EDOT/AuNTs presented a potential of −35 mV, confirming that the micellar systems are stable, even after the addition of the monomer and the nanoparticles.

In Figure 1b,c, it can be seen that the κC and κC/EDOT dispersion showed a monodisperse particle size distribution, which may be attributed to the κC micelles, similar to previous reports (Gu, Decker, & McClements, 2005; Hernandez-Suarez et al., 2019). By means of DLS measurements, the dispersion system, constituted by κC/EDOT/AuNTs, showed two populations at 26 and 231 nm in size (Figure 1d). The dispersion formed was stable and the values were similar to those reported for nanoparticle systems (Chen et al., 2018).

2.1.3 | Modified electrode characterization

The composition of the conductive coating was monitored by FTIR and Raman spectroscopy analysis in order to determine the presence of the compounds of interest (PEDOT/κC/AuNTs). The main signals found for the composite coating are summarized in Table S1.

The conductive polymer showed a strong signal around 1,461 cm^{-1} in the Raman spectra, absent in the FTIR analysis, which is related to the thiophene ring (Figures S3 and S4). Some characteristic bands for the doping agent (κC) were observed at 3,400 and 1646 cm^{-1} using FTIR analysis (Figure S4). The AChE enzyme presents typical bands in the spectral ranges 600–1800 cm^{-1} and 2500–3120 cm^{-1} (Figure S5). Nonetheless, the enzyme signals were overlapped by the PEDOT/κC spectrum in the composite and by the buffer in the case of soluble enzyme (Figure S6).

The spectra of AChE (Figure S5) matched to typical bands for enzymes, the one at 950 cm^{-1} is attributed to the C-N bending stretching vibration, the signal at 1,267 cm^{-1} corresponds to the rocking vibration of the methyl group and the signal at 1,438 cm^{-1} is attributed to symmetric deformation motions within the methyl groups (El Alami, Lagarde, Tamer, Baitoul, & Daniel, 2016). Even though, the components showed the characteristic signals for proteins, the direct identification of the enzyme in the conductive matrix was not achieved by single measurement of FTIR. Therefore, a Raman confocal scan was performed in a 2 μm^2 area and 0.5 μm depth. The relative intensity of the band at 1,640 cm^{-1}, associated with the amide-I group (see Table S1), is shown in Figure S7. The areas with amide bands may be identified from this Raman image and appear as bright yellow areas. The analysis of the 3D peak region thus provides a sight of the enzyme distribution inside of the conductive layer. Finally, the activity of the anchored enzyme into the conductive layer was measured using cyclic voltammetry (see section 2.2).

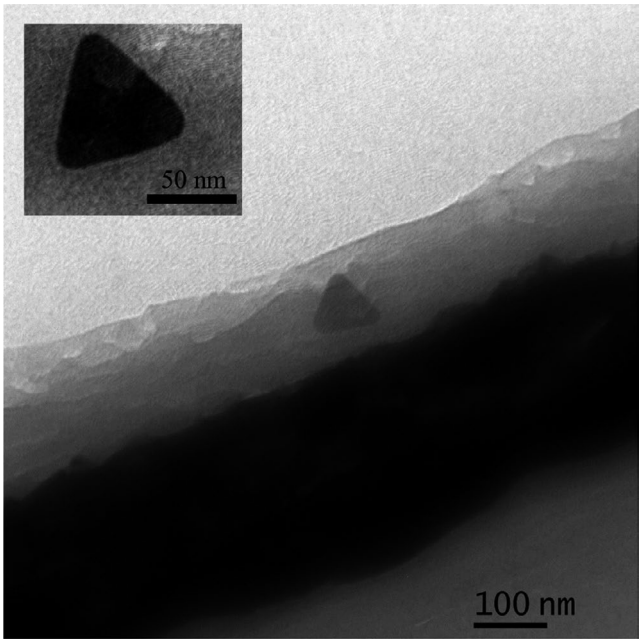

FIGURE 2 TEM micrograph of gold nanoparticles inside the conductive polymer, electrodeposited on a flexible gold electrode

In order to confirm the presence of AuNTs in the conductive layer, transmission electron microscopy (TEM) was performed. In the TEM image (Figure 2), a triangular shaped particle, around 65 nm size and surrounded by the conductive polymer, was identified.

The topographic image of the conductive coat surface was obtained using atomic force microscopy (AFM). An irregular surface topology is observed (see Figure 3a), due to the micellar polymerization process previously reported (Hernandez-Suarez et al., 2019). Furthermore, deformation and adhesion values confirmed the mechanical properties associated with the soft PEDOT coat. Nevertheless, the electrical image (by PeakForce-TUNA) revealed a difference in the conductivity associated with the gold particles in the polymer coat. Higher positive current (Figure 3d) was observed in some specific areas, matching the gold nanoparticle shape and size observed by TEM in Figure 2. Figure S2 shows that the gold nanoparticles have a triangular shape with side length of approximately 60 nm. Even though the particles are partially occluded in the conductive polymer, since they are not directly observed on the electrode surface, its electroactivity was confirmed by AFM and electrochemical studies.

2.1.4 | Electrochemical characterization of PEDOT/κC/AuNTs/AChE and bare gold electrodes

Cyclic voltammetric (CV) experiments were performed in order to study the electrochemical behaviour of the modified electrodes and

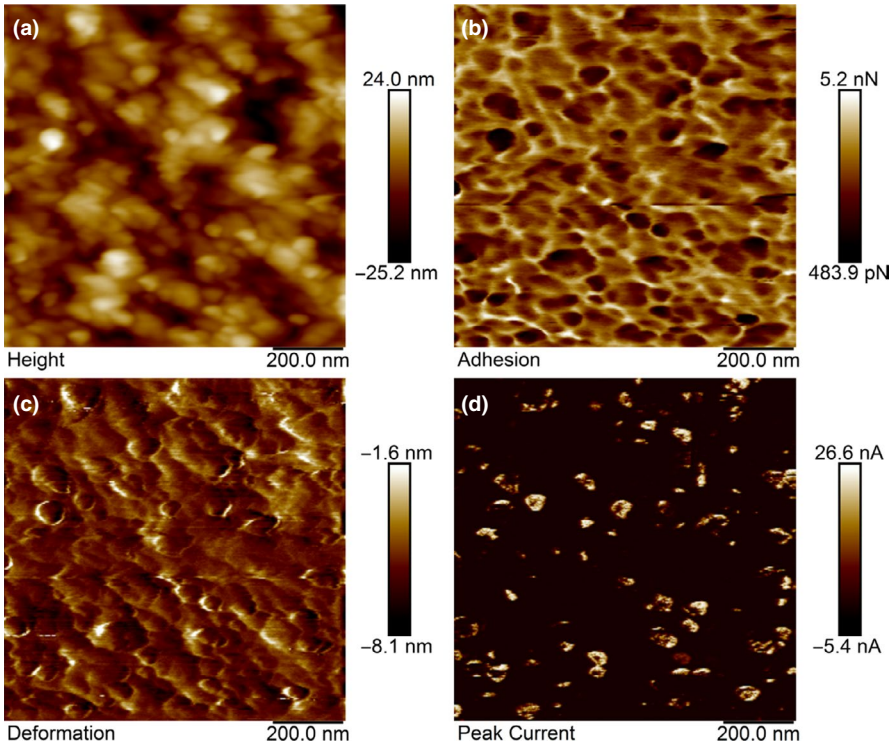

FIGURE 3 AFM images of a conductive PEDOT coat modified with AuNTs. (a) Topography, (b) adhesion, (c) deformation and (d) PF-TUNA

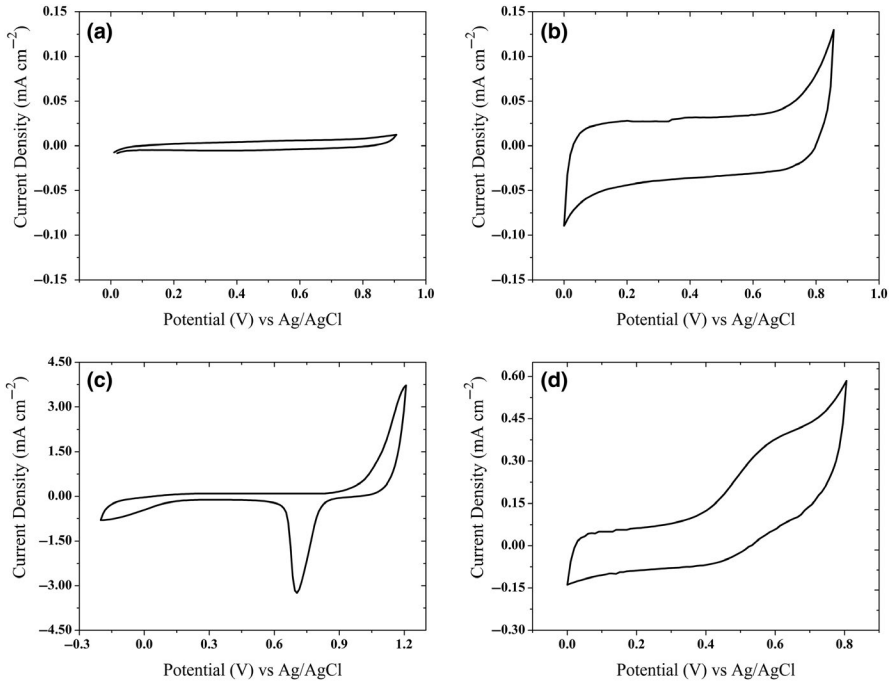

FIGURE 4 Cyclic voltammograms obtained at 50 mV/s for (a) gold electrode in Britton Robinson buffer, (b) PEDOT/κC/AuNTs/AChE modified electrode in Britton Robinson buffer, (c) PEDOT/κC/AuNTs/AChE modified electrode in H_2SO_4 (0.5 M) and (d) PEDOT/κC/AuNTs modified electrode in the presence of N-acetyl cysteine 1.25 mM in Robinson Britton buffer

the enzymatic activity. The CV of bare gold electrodes (Figure 4a) shows a typical behaviour for metal electrodes in solution. Meanwhile, the PEDOT/κC/AuNTs/AChE electrode voltammogram shows an increase in the hysteresis (Figure 4b), due to the increment in the surface area caused by the PEDOT and AuNTs, providing better electrical connection between the electrode active sites and making the electron transfer easier (Wei & Wang, 2015; Wen et al., 2012). The gold nanoparticles behaviour inside the conductive coat was studied performing a CV sweeping in H_2SO_4 (0.5 M). Redox peaks that appear in Figure 4c, agreed with the typical gold electrochemical behaviour that has been widely reported (El Wakkad & Shams El Din, 1954; Koryta & Pradáč, 1968; Maringa, Antunes, & Nyokong, 2014). The oxidation signal close to 1.2 V is linked to a gold pre-oxide zone producing Au(OH) (El Wakkad & Shams El Din, 1954). During the reverse scan, a reduction signal at 0.7 V (El Wakkad & Shams El Din, 1954) confirms the electrochemical activity of the gold nanoparticles in the PEDOT/κC/AuNTs modified electrode.

Figure 4d shows the N-acetyl cysteine oxidation signal at 0.60 V in the cyclic voltammogram of the modified electrode. Cysteine is generally used in the determination of sulfhydryl groups (SH) by a non-reversible electrochemical oxidation (Davis & Blanco, 1966; Wang & Huang, 2012). Therefore, this electrochemical reaction is used to identify the production of thiocholine (ATCh) by the AChE enzyme (Maleki, Safavi, Sedaghati, & Tajabadi, 2007), the current at that potential is used to quantify the enzyme activity.

2.2 | Enzymatic activity measurement

The activity of the immobilized enzyme in the PEDOT/κC/AuNTs/AChE electrode was monitored by electrochemical analysis using 2 mM ATCh. The bioactivity of the entrapped AChE was determined by measuring the oxidation of thiocholine, an enzymatic product obtained from ATCh hydrolysis. Table S2 shows the measured current, obtained from the enzymatic reaction occurring at the working electrode surface, at 0.65 V.

Although the specific incorporation mechanism of molecules in the growing PEDOT/κC matrix is not yet fully understood (Ahuja, Mir, & Kumar, 2007), the enzyme anchoring during the electrodeposition ensures proximity between the active site of the enzyme and the conducting surface of the electrode (Liu, Wen, et al., 2011). Through this strategy, it is possible to reduce the amount of enzyme during the electrode preparation, compared to other similar reports (Gong, Liu, Song, Zhang, & Zhang, 2009; Hou, Ou, Chen, & Wu, 2012). Besides, due to its high sensibility, AChE enzyme is one of the most utilized biomarkers for detection of organophosphates in biosensors. Its stability and possibility of reusing the immobilization system have also been studied in previous publications (Ardao, Ramírez-Sánchez, Cadavid, Starbird-Pérez, & Loza, 2018; Liu, Su, et al., 2011).

2.3 | Inhibition assays

The concentration of Chlorpyrifos was detected by inhibition of the enzyme directly entrapped into the conductive layer even in enriched real samples. The inhibition effect of the enzyme was studied using 10 mg/ml Chlorpyrifos solution, showing an inhibition percentage of 27.1 ± 4.3% at 5 min of the enzymatic reaction. In general, the inhibition percentage for the 10 mg/ml Chlorpyrifos sample remained constant at 5 and 10 min of reaction, confirming that the pesticide acts as an irreversible inhibitor (Ramírez-Sánchez, Alvarado-Hidalgo, Ardao, & Starbird-Pérez, 2018; Zhang, Asiri, Liu, Du, & Lin, 2014). In order to evaluate the performance of our system, two real samples were measured: a lagoon sample (Madre de Dios), situated near agricultural activities and a river sample from the Purires River, both localized in Costa Rica.

The Madre de Dios lagoon sample was studied by gas chromatography and liquid chromatography (see Table S3) to quantify the effect of the interferences in a real sample. In Table S3 is summarized the concentration of some of the studied components, showing that none of them are detectable, or, they are at a trace level. The absence of inhibition effect when the lagoon sample was tested, confirmed the outstanding performance of the biosensor in real conditions. Then, a 15 mg/ml solution was used to enrich the river and lagoon water samples and less than 10% of enzyme activity was found in both samples, similar has been reported with the same amount of pesticide (Davis, Anderson, & Pope, 2016). Table 1 shows the calculated inhibition percentage for the evaluated samples.

In accordance with the IC_{50} reported value, a Chlorpyrifos concentration lower than 0.35 mg/ml has no significant effect in the cholinesterase activity (Food and Agriculture Organization & World Health Organization, 2004). However, a 70% of inhibition of the AChE activity is considered to be harmful to human health, according to the Biologic Limit Values (BLV) (Food and Agriculture Organization & World Health Organization, 2004). Therefore, this composite coat (PEDOT/κC/AuNTs/AChE) provides a suitable method to be used in the study of the bioavailability of pesticides in water during environmental monitoring.

3 | CONCLUSIONS

A novel electrochemical active layer was used to anchor the AChE enzyme for bioelectronic devices. AuNTs were homogeneously dispersed in the PEDOT layer, improving the electrochemical response of the enzymatic activity. The incorporation of AuNTs and the strategy of enzyme immobilization enabled the construction of a suitable biosensor for the detection of Chlorpyrifos. The inhibition of the enzyme revealed a correlation with the concentration of pesticide in water, showing a suitable response at 10 mg/ml Chlorpyrifos concentration. The outstanding performance of the AChE biosensor

TABLE 1 Percentage of inhibition of AChE related to the pesticide concentration

Measurement	Reaction time (min)	Pesticide concentration (mg/ml)	Inhibition (%)
Inhibitory assay	5	10.0 ± 0.1	27.1 ± 4.3
	10	10.0 ± 0.1	22.9 ± 4.3
Lagoon water sample	5	<2.0E−5[a]	0.0
Enriched river water sample	5	15.0 ± 0.2	92.4
Enriched lagoon water sample	5	15.0 ± 0.2	88.32

[a]Chlorpyrifos concentration was lower than the limit of detection (LOD) using LCMSM/GCMS.

suggests that it may be taken into the field for environmental monitoring of water supplies from agriculturally based countries. Finally, the composite layer may be tunable to entrap other enzymes and incorporate different nanoparticles in order to be applied to alternative systems in the medical and environmental field.

4 | EXPERIMENTAL SECTION

4.1 | Materials

3,4-ethylenedioxythiophene (EDOT, 97% purity), Spurr® low viscosity resin, acetylcholine chloride (ATCh, 99% purity), potassium chloride, κ-carrageenan (κC), acetylcholinesterase (AChE) from *Electrophorus electricus* (E.C 3.1.1.7, 500 U/ml), acetylcysteine, 5,5′-dithiobis(2-nitrobenzoic acid) (Ellman reagent, 98% purity), sodium acetate anhydrous (99% purity), potassium chloride (KCl, 99% purity), glacial acetic acid (CH_3CO_2H), boric acid (H_3BO_3, 99% purity) were purchased from Sigma-Aldrich. Sodium hydroxide (NaOH, 98% purity) was obtained from Macron fine chemicals; phosphoric acid (H_3PO_4) was purchased from Eltee International. The gold nanoparticle precursor ($HAuCl_4$) was obtained from Sigma-Aldrich. The phospholipids, 1,2-dimyristoyl-sn-glycero-3-phospho-rac-glycerol, sodium salt (DMPG-Na) and the phosphatidylcholine (PC) were donated by LIPOID AG.

4.2 | Synthesis and purification of the gold nanoparticles

Gold nanotriangles (AuNTs) were synthesized in a vesicle template phase of the mixed phospholipids DMPG-Na (5 mg) and PC (5 mg) in 10 ml of water. Subsequently, 1 ml of the dispersion was sonicated for 1 min, and the resulting transparent vesicle dispersion was mixed with 0.250 ml of the freshly prepared aqueous 2 mM tetrachloroaurate precursor solution. The mixtures were gently stirred at 25°C overnight resulting in dark red coloured clear dispersion. After the reaction was completed, the AuNPs were collected and centrifuged (5,702, Eppendorf™) for 1 hr at 2,056 *g*. The supernatant was removed, and the particles were redispersed in water. The procedure was performed twice. Further, the separation of gold nanotriangles (AuNTs) from remaining spherical particles were performed by adding surfactant micelles to the mixture, which induce depletion interaction between the colloidal particles (Park, Koerner, & Vaia, 2010). Then, to 1 ml of the mixed gold solution 1 ml of surfactant SDS of 0.150 M was added without stirring. The flocculation was complete overnight, the supernatant was removed, and the precipitated nanoparticles were washed and redispersed in deionized water.

4.3 | PEDOT/κC/AuNTs/AChE working electrode modification

Gold nanotriangles (AuNTs) were synthesized in a vesicle template phase of the mixed phospholipids. Electrodes were fabricated by the deposition of gold on a polyimide substrate, using a shadow mask, and an exposed active area of the electrode, was polymerized according to a previous work (Starbird et al., 2012). The polymer (PEDOT) was deposited from its monomer form (EDOT 10 mM), dispersed along with AuNTs (ca. 1.07E + 9 particles/ml) and 2.5 U/ml acetylcholinesterase in a κ-carrageenan 0.4% m/v dispersion adjusted to pH 7.4. The solution was electropolymerized at 30°C under galvanostatic conditions with an Autolab Potentiostat supplied by Metrohm (PGSTAT-302N, AUTOLAB) with a fixed charge density of 60 mC/cm^2. Finally, after the electropolymerization, the electrode was washed with distilled water and stored at 4°C in Robinson Britton buffer solution.

4.4 | Dispersion characterization

The hydrodynamic diameter and ζ-potential of the dispersions were measured using a Zetasizer instrument (Nano ZS, Malvern Panalytical Ltd.). All measurements were performed at 25°C and 173° angle, after high-power ultrasound treatment of the samples using a Sonifier QSonica (Q700, Ultrasonic Corporation).

4.5 | Characterization of PEDOT/κC/AuNTs/AChE and bare gold electrodes by Cyclic voltammetry

EDOT/κC/AuNTs/AChE and bare gold electrodes were incubated for 5 min with Robinson Britton buffer, pH 7 and using a three-electrode configuration with Ag|AgCl (3.0 M KCl) as reference electrode and gold as counter electrode (Figure S1). The cyclic voltammetry (CV) measurements were carried out at 0.05 V/s scan rate in different solutions.

4.6 | Nanomechanical characterization Peak Force TUNA

Surface topography and electrical conductivity were obtained simultaneously using an atomic force microscope (AFM) (MultiMode 8, Bruker) operating in Peak force tunnelling mode (PF-TUNA) at room conditions. The cantilevers are PF-TUNA probe (Bruker AFM Probes) with a resonant frequency around 70 KHz and spring constant of 0.4 N/m and a Pt/Ir tip coating. A 1 V DC bias is applied between the sample and the electrically conductive tip and a linear current amplifier, with a range of 1 pA/V to 100 nA/V, was used for sensing the current passing through the sample. The images were studied using the software NanoScope Analysis (version 1.80, Bruker 8).

4.7 | Transmission electron microscopy

PEDOT/AuNPs/κC/AChE coats were passed through a transition solvent process and embedded into a Spurr® low viscosity resin. After embedding the samples, the resin block was thin

sectioned (50–70 nm) using a Leica Ultramicrotome (EM UC7, Leica Microsystems) with the samples being collected on a metal grid for transmission electron microscopy (TEM) observation. The images were recorded in a TEM (JEM 2011, Jeol) at 200 kV.

4.8 | Infrared and Raman spectroscopy

Attenuated total reflectance–Fourier transformed infrared spectroscopy (ATR-FTIR) was conducted on a spectrometer equipped with an iATR accessory (Nicolet 380, Thermo Scientific) controlled with OMNIC v9.3.30 software. Dry samples were placed directly onto the diamond window (ca. 2 mg) without further preparation. Measurements were made in absorbance mode, in the 4000–450 cm^{-1} spectral range using 64 scans at a resolution of 2 cm^{-1}. Raman spectroscopy was conducted using a confocal Raman microscope (Alpha300 R WITec, GmbH) with a 532 nm excitation laser, exposure time of 0.5 s and 100 accumulations. The Raman stack scan was obtained using an integration time of 4 s in a 2 μm^2 area; 20 measurements per line were recorded for a total of 20 lines in each stack. The scan depth was fixed at 0.5 μm and a total of 10 stack scans were achieved. Oversampling was used to improve the image quality, which was done in case of the cross-sectional scan. The intensity of the relative wavenumber at 1,640 cm^{-1} (related to amines I groups see Table S2) was extracted from each acquired spectrum and plotted as a map in Figure S7.

4.9 | Enzymatic activity evaluation of immobilized AChE

Electrochemical measurements of immobilized AChE were carried out by CV using the three electrodes system. The response of the trapped enzyme in presence of the substrate was determined by the thiol group oxidation of thiocholine at 37.0 ± 0.5°C and pH 7. CV measurements were carried out by scanning from −0.2 to 0.85 V with a 0.05 V/s scan rate. A calibration curve of thiol oxidation in CV measurements was previously performed using N-acetyl cysteine as a standard.

For the inhibitory assays, the electrode with trapped enzyme was pre-incubated, for ten minutes, in the continuous flow cell with a solution of 10 mg/ml standard Chlorpyrifos pesticide in Robinson Britton buffer solution, 1 M, pH 7 at room temperature. After incubation, ATCh 2 mM was added into the cell. For the enzymatic activity measurements, the same procedure as described above was performed. The enzymatic reactions with and without pesticides were performed by triplicate.

An electrode with immobilized AChE was pre-incubated, for 5 min (Ramírez-Sánchez et al., 2018) in lagoon and river water samples (see Supporting information) enriched with Chlorpyrifos 15 mg/ml, in the continuous flow cell, to evaluate the inhibitory effect from the pesticide. After incubation, the measurements were carried out in Robinson Britton buffer solution 1 M, pH 7 at room temperature.

4.10 | Real sample analysis

Pesticide determination, in the present study, was measured in two water samples. One, the lagoon water (Madre de Dios) (Global Positioning System (GPS) coordinates: latitude: 10.1921, longitude: −83.2954), a lagoon situated near agricultural activities. The second sample was obtained in the Purires River, located in El Guarco, Tobosi, Cartago (GPS): latitude: 9.84858, longitude: −83.9632). This river presents agricultural activities in its surroundings.

The pesticide concentration in the lagoon sample was analysed using two techniques: gas chromatography with mass detector (GC-MS) (7890, Agilent) and liquid chromatography with mass detector (UPLC-MS/ MS) (XEVO T -QS Micro, Waters). In both cases using a solid-phase extraction (SPE), the extract in isooctane was analysed by gas chromatography with mass detector 5975C, with an automatic CTC-Combipal reader and coupled in the Chemical program for data acquisition in selective monitoring mode (SIM) and scanning mode (TIC). The analytical column used was a BPX 35 (30 m × 0.25 mm × 0.25 μm) (SGE, USA) with a programmed temperature profile and helium as carrying gas. The injection volume was 2 μl in splitless mode for 60 s. For the UPLC, the water sample was extracted by solid-phase extraction (SPE). An Isolute ENV + cartridge (200 mg/6 ml), previously conditioned, was used. The sample was shaken and passed through the cartridge. The cartridge was dried and eluted with only methanol or with methanol and then ethyl acetate. The extract was concentrated to methanol/water (10:90 V/V or 40:60 V/V). The final volume of the extract was around 0.5 ml. The analytical column used was a BEH C18 1.7 μm, 2.1 mm × 100 mm (Water), at 45°C. A mobile phase was applied to the system consisting of water with 0.1% formic acid and 1 mM ammonium acetate and B methanol with 0.1% formic acid and 1 mM ammonium acetate and with a total flow of 0.4 ml/min; the automatic reader was set up at 10.0 ± 0.1°C and the injection volume was 5 μl. The pesticides included in the two methods were identified and quantified by injecting pesticide standards and different calibration curves.

ACKNOWLEDGEMENTS

This work was financially supported by FEES funding (CONARE) Grant number 08-2018 and Instituto Tecnológico de Costa Rica (ITCR). Roy Zamora-Sequeira would like to thank the Technology Bureaus of Costa Rica (MICITT and CONICIT) and National Learning Institute (INA) for the scholarship provided during this project. Luis Alvarado and Alejandro Medaglia from the Laboratorio Institucional de Microscopía at ITCR for the preparation of the TEM samples, Ing. Rulio Guerrero Barrantes from CICIMA for his support in the spectroscopy acquisition data and Evelyn Ruiz Albuquerque for her participation in the electrode fabrication process. Finally, we would like to thank Diana Robles from the Research Center and Chemical and Microbiological Services (CEQIATEC). RGSF-RIP.

CONFLICT OF INTEREST

The authors declare no competing interests.

ORCID

Karla Ramírez-Sánchez https://orcid.org/0000-0001-5219-9646
Fernando Alvarado-Hidalgo https://orcid.org/0000-0002-7352-5292
Roy Zamora-Sequeira https://orcid.org/0000-0002-9356-8978
Giovanni Sáenz-Arce https://orcid.org/0000-0003-1848-7980
Oscar Rojas-Carrillo https://orcid.org/0000-0003-1305-7615
Esteban Avedaño-Soto https://orcid.org/0000-0001-5500-3821
Clemens Ruepert https://orcid.org/0000-0001-5109-2222
Freylan Mena-Torres https://orcid.org/0000-0002-1215-0378
Ricardo Starbird-Pérez https://orcid.org/0000-0002-0700-0594

REFERENCES

Ahuja, T., Mir, I. A., Kumar, & D., Rajesh (2007). Biomolecular immobilization on conducting polymers for biosensing applications. *Biomaterials*, *28*, 791–805.

Ardao, I., Ramírez-Sánchez, K., Cadavid, M. I., Starbird-Pérez, R., & Loza, M. I. (2018). Acetylcholinesterase immobilization on microplates for high-throughput screening of inhibitors. *Conf. Basic Clin. Pharmacol. Toxicol.*, *123*, 62.

Bollella, P., Hibino, Y., Conejo-Valverde, P., Soto-Cruz, J., Bergueiro, J., Calderón, M., … Gorton, L. (2019). The influence of the shape of Au nanoparticles on the catalytic current of fructose dehydrogenase. *Analytical and Bioanalytical Chemistry*, *1*, 1–13. https://doi.org/10.1007/s00216-019-01944-6

Chen, N., Liu, H., Zhang, Y., Zhou, Z., Fan, W., Yu, G., … Wu, A. (2018). A colorimetric sensor based on citrate-stabilized AuNPs for rapid pesticide residue detection of terbuthylazine and dimethoate. *Sensors and Actuators B: Chemical*, *255*, 3093–3101.

Davis, D., Anderson, T., & Pope, C. (2016). Inhibition of acetylcholinesterase in the anaxyrus cognatus liver by chlorpyrifos oxon. *Reports from Life Sci. Freshmen Res. Sch*, *2*, 1–5.

Davis, D. G., & Blanco, E. (1966). An electrochemical study of the oxidation of L-cysteine. *Journal of Electroanalytical Chemistry*, *12*, 254–260.

Dorraki, N., Safa, N. N., Jahanfar, M., Ghomi, H., & Ranaei-Siadat, S. O. (2015). Surface modification of chitosan/PEO nanofibers by air dielectric barrier discharge plasma for acetylcholinesterase immobilization. *Applied Surface Science*, *349*, 940–947.

Du, D., Chen, S., Cai, J., & Zhang, A. (2007). Immobilization of acetylcholinesterase on gold nanoparticles embedded in sol–gel film for amperometric detection of organophosphorous insecticide. *Biosensors & Bioelectronics*, *23*, 130–134. https://doi.org/10.1016/j.bios.2007.03.008

El Alami, A., Lagarde, F., Tamer, U., Baitoul, M., & Daniel, P. (2016). Enhanced Raman spectroscopy coupled to chemometrics for identification and quantification of acetylcholinesterase inhibitors. *Vibrational Spectroscopy*, *87*, 27–33.

El Wakkad, A. M., & Shams El Din, A. M. (1954). The anodic oxidation of metals at very low current density. Part V. Gold. *Journal of the Chemical Society (Resumed)*, *1*, 3098–3102.

Food and Agriculture Organization (2017). *Agri-environmental indicators pesticides*. Retrieved from http://www.fao.org/faostat/en/#data/EP

Food and Agriculture Organization & World Health Organization (2004). *Chlorpyrifos in drinking-water. Background document for development of WHO guidelines for drinking-water quality*. Geneva, Switzerland: World Health Organization (WHO/SDE/WSH/03.04/33).

Goding, J. A., Gilmour, A. D., Martens, P. J., Poole-Warren, L. A., & Green, R. A. (2015). Small bioactive molecules as dual functional co-dopants for conducting polymers. *Journal of Materials Chemistry B*, *3*, 5058–5069.

Gong, J., Liu, T., Song, D., Zhang, X., & Zhang, L. (2009). One-step fabrication of three-dimensional porous calcium carbonate–chitosan composite film as the immobilization matrix of acetylcholinesterase and its biosensing on pesticide. *Electrochemistry Communications*, *11*, 1873–1876.

Gu, Y. S., Decker, E. A., & McClements, D. J. (2005). Influence of pH and carrageenan type on properties of β-lactoglobulin stabilized oil-in-water emulsions. *Food Hydrocolloids*, *19*, 83–91.

Hernandez-Suarez, P., Ramirez, K., Alvarado, F., Avendano, E., & Starbird, R. (2019). Electrochemical characterization of poly (3,4-ethylenedioxythiophene)/κ-carrageenan as a biocompatible conductive coat for biologic applications. *MRS Communications*, *9*, 218–223.

Hou, S., Ou, Z., Chen, Q., & Wu, B. (2012). Amperometric acetylcholine biosensor based on self-assembly of gold nanoparticles and acetylcholinesterase on the sol–gel/multi-walled carbon nanotubes/choline oxidase composite-modified platinum electrode. *Biosensors & Bioelectronics*, *33*(1), 44–49. https://doi.org/10.1016/j.bios.2011.12.014

Kaur, G., Adhikari, R., Cass, P., Bown, M., & Gunatillake, P. (2015). Electrically conductive polymers and composites for biomedical applications. *RSC Advances*, *5*, 37553–37567.

Kim, D.-H., Richardson-Burns, S. M., Hendricks, J. L., Foster, B., Martin, D. C., & Povlich, L. K. (2007). Polymerization of the conducting polymer poly (3,4-ethylenedioxythiophene) (PEDOT) around living neural cells. *Biomaterials*, *28*, 1539–1552.

Kok, F. N., & Hasirci, V. (2004). Determination of binary pesticide mixtures by an acetylcholinesterase–choline oxidase biosensor. *Biosensors and Bioelectronics*, *19*, 661–665.

Koryta, J., & Pradáč, J. (1968). Electrode processes of the sulfhydryl-disulfide system. *Journal of Electroanalytical Chemistry and Interfacial Electrochemistry*, *17*, 185–189.

Liebig, F., Thünemann, A. F., & Koetz, J. (2016). Ostwald ripening growth mechanism of gold nanotriangles in vesicular template phases. *Langmuir*, *32*, 10928–10935.

Liu, M., Wen, Y. P., Xu, J. K., He, H. H., Li, D., Yue, R. R., & Liu, G. D. (2011). An amperometric biosensor based on ascorbate oxidase immobilized in poly (3,4-ethylenedioxythiophene)/multi-walled carbon nanotubes composite films for the determination of L-ascorbic acid. *Analytical Sciences*, *27*, 477.

Liu, T., Su, H., Qu, X., Ju, P., Cui, L., & Ai, S. (2011). Acetylcholinesterase biosensor based on 3-carboxyphenylboronic acid/reduced graphene oxide-gold nanocomposites modified electrode for amperometric detection of organophosphorus and carbamate pesticides. *Sensors and Actuators B: Chemical*, *160*(1), 1255–1261. https://doi.org/10.1016/j.snb.2011.09.059

Maleki, N., Safavi, A., Sedaghati, F., & Tajabadi, F. (2007). Efficient electrocatalysis of l-cysteine oxidation at carbon ionic liquid electrode. *Analytical Biochemistry*, *369*, 149–153.

Mandal, N., Bhattacharjee, M., Chattopadhyay, A., & Bandyopadhyay, D. (2019). Point-of-care-testing of α-amylase activity in human blood serum. *Biosensors & Bioelectronics*, *124–125*, 75–81.

Mantione, D., del Agua, I., Sanchez-Sanchez, A., & Mecerreyes, D. (2017). Poly (3,4-ethylenedioxythiophene) (PEDOT) derivatives: Innovative conductive polymers for bioelectronics. *Polymers (Basel)*, *9*, 354. https://doi.org/10.3390/polym9080354

Maringa, A., Antunes, E., & Nyokong, T. (2014). Electrochemical behaviour of gold nanoparticles and Co tetraaminophthalocyanine on glassy carbon electrode. *Electrochimica Acta*, *121*, 93–101.

Park, K., Koerner, H., & Vaia, R. A. (2010). Depletion-induced shape and size selection of gold nanoparticles. *Nano Letters*, *10*, 1433–1439.

Pumera, M. (2014). *Nanomaterials for electrochemical sensing and biosensing*. Singapore: Pan Stanford Publishing Pte. Ltd.

Ramírez-Sánchez, K., Alvarado-Hidalgo, F., Ardao, I., & Starbird-Pérez, R. (2018). Enzymatic inhibition constant of acetylcholinesterase for the electrochemical detection and sensing of Chlorpyrifos. *Journal of Natural Resources and Development*, *8*, 9–14. https://doi.org/10.5027/jnrd.v8i0.02

Ren, S., Gong, C., Zeng, P., Guo, Q., & Shen, B. (2016). Synthesis of flammulina-like mordenite using starch as template and high catalytic performance in crack of wax oil. *Fuel*, *166*, 347–351.

Schulze, H., Schmid, R. D., & Bachmann, T. T. (2004). Activation of phosphorothionate pesticides based on a cytochrome P450 BM-3 (CYP102 A1) mutant for expanded neurotoxin detection in food using acetylcholinesterase biosensors. *Analytical Chemistry*, *76*, 1720–1725.

Starbird, R., Bauhofer, W., Meza-Cuevas, M., & Krautschneider, W. H. (2012). *Effect of experimental factors on the properties of PEDOT-NaPSS galvanostatically deposited from an aqueous micellar media for invasive electrodes*. The 5th 2012 Biomedical Engineering International Conference. BMEiCON 2012.

Stoilova, O., Manolova, N., Gabrovska, K., Marinov, I., Godjevargova, T., Mita, D. G., & Rashkov, I. (2010). Electrospun polyacrylonitrile nanofibrous membranes tailored for acetylcholinesterase immobilization. *Journal of Bioactive and Compatable Polymers*, *25*, 40–57.

Sun, X., & Wang, X. (2010). Acetylcholinesterase biosensor based on Prussian blue-modified electrode for detecting organophosphorous pesticides. *Biosensors & Bioelectronics*, *25*, 2611–2614.

Wang, B., Akiba, U., & Anzai, J. I. (2017). Recent progress in nanomaterial-based electrochemical biosensors for cancer biomarkers: a review. *Molecules*, *22*, 1048. https://doi.org/10.3390/molecules22071048

Wang, L. H., & Huang, W. S. (2012). Electrochemical oxidation of cysteine at a film gold modified carbon fiber microelectrode its application in a flow—through voltammetric sensor. *Sensors*, *12*, 3562–3577.

Wei, M., & Wang, J. (2015). A novel acetylcholinesterase biosensor based on ionic liquids-AuNPs-porous carbon composite matrix for detection of organophosphate pesticides. *Sensors and Actuators B: Chemical*, *211*, 290–296.

Wen, Y., Xu, J., Liu, M., Li, D., Lu, L., Yue, R., & He, H. (2012). A vitamin C electrochemical biosensor based on one-step immobilization of ascorbate oxidase in the biocompatible conducting poly(3,4-ethylenedioxythiophene)-lauroylsarcosinate film for agricultural application in crops. *Journal of Electroanalytical Chemistry*, *674*, 71–82.

Zamora-Sequeira, R., Ardao, I., Starbird, R., & García-González, C. A. (2018). Conductive nanostructured materials based on poly-(3,4-ethylenedioxythiophene) (PEDOT) and starch/κ-carrageenan for biomedical applications. *Carbohydrate Polymers*, *189*, 304–312.

Zhang, W., Asiri, A. M., Liu, D., Du, D., & Lin, Y. (2014). Nanomaterial-based biosensors for environmental and biological monitoring of organophosphorus pesticides and nerve agents. *Trends in Analytical Chemistry*, *54*, 1–10.

SUPPORTING INFORMATION

Additional supporting information may be found online in the Supporting Information section.

How to cite this article: Ramírez-Sánchez K, Alvarado-Hidalgo F, Zamora-Sequeira R, et al. Biosensor based on the directly enzyme immobilization into a gold nanotriangles/conductive polymer biocompatible coat for electrochemical detection of Chlorpyrifos in water. *Med Devices Sens*. 2019;2:e10047. https://doi.org/10.1002/mds3.10047